Preclinical Testing of Chronic ICA-1S Exposure: A Potent Protein Kinase C-ι Inhibitor as a Potential Carcinoma Therapeutic

Christopher A. Apostolatos [1,†]**, Wishrawana S. Ratnayake** [1,†]**, Sloan Breedy** [1]**, Jacqueline Kai Chin Chuah** [2]**, James Alastair Miller** [3]**, Daniele Zink** [4]**, Marie Bourgeois** [5] **and Mildred Acevedo-Duncan** [1,*]

1. Department of Chemistry, University of South Florida, 4202 E. Fowler Ave. CHE 205, Tampa, FL 33620, USA; capostolatos@usf.edu (C.A.A.); ratnayake@usf.edu (W.S.R.); sbreedy@usf.edu (S.B.)
2. Cellbae Pte Ltd., 61 Science Park Road, #03-07/08, The Galen, Singapore 117525, Singapore; jacqueline@cellbae.com
3. Bioinformatics Institute, Agency for Science, Technology, and Research (A*STAR), 30 Biopolis Street, #07-01 Matrix, Singapore 138671, Singapore
4. NanoBio Lab, Agency for Science, Technology, and Research (A*STAR), 31 Biopolis Way, The Nanos, #09-01, Singapore 138669, Singapore
5. College of Public Health, University of South Florida, Tampa, FL 33620, USA; mmbourge@usf.edu
* Correspondence: macevedo@usf.edu; Tel.: +(813)-748-4715
† These authors contributed equally to this work.

Abstract: Protein kinase C-iota (PKC-ι) is an oncogene overexpressed in many cancer cells including prostate, breast, ovarian, melanoma, and glioma cells. Previous in vitro studies have shown that 5-amino-1-((1R,2S,3R,4R)-2-3-dihydroxy-4-(hydroxymethyl)cyclopentyl)-1H-imidazole-4-carboxamide (ICA-1S), a PKC-ι-specific inhibitor, has low toxicity in both acute and sub-acute mouse model toxicological testing and is an effective therapeutic against several cancer cell lines showing significant reductions in tumor growth when treating athymic nude mice with xenografted carcinoma cell lines. To further assess ICA-1S as a possible therapeutic agent, chronic mouse model toxicological testing was performed in vivo to provide inferences concerning the long-term effects and possible health hazards from repeated exposure over a substantial part of the animal's lifespan. Subjects survived well after 30, 60, and 90 days of doses ranging from 50 mg/kg to 100 mg/kg. Heart, liver, kidney, and brain tissues were then analyzed for accumulations of ICA-1S including the measured assessment of aspartate transaminase (AST), alkaline phosphatase (ALK-P), gamma-glutamyl transferase (GGT), troponin, and C-reactive protein (CRP) serum levels to assess organ function. Predictive in vitro/in silico methods were used to predict compound-induced direct hepatocyte toxicity or renal proximal tubular cell (PTC) toxicity in humans based on the high-content imaging (HCI) of compound-treated cells in combination with phenotypic profiling. In conclusion, ICA-1S shows low toxicity in both acute and chronic toxicology studies, and shows promise as a potential therapeutic.

Keywords: PKC-ι; specific inhibition; acute and chronic toxicity

1. Introduction

Protein kinase C-iota (PKC-ι), an oncogene that plays a role in the effectiveness of 5-amino-1-((1R,2S,3R,4R)-2-3-dihydroxy-4-(hydroxymethyl)cyclopentyl)-1H-imidazole-4-carboxamide (ICA-1S), is overexpressed in several cancers including prostate, breast, ovarian, melanoma, and glioma [1–5]. Conditions that can lead to the overexpression of PKC-ι include the loss or mutation of the phosphatase and tensin homolog (PTEN) and/or the over-activation of phosphatidylinositol 3–kinase (PI3K) [6]. These mutations, which are resistant to T-cell-mediated apoptosis, are associated with the NF-κB pathway where PKC-ι assists in the translocation of NF-κB to the nucleus [7]. Prior studies also suggest that PKC-ι is associated with the epithelial-to-mesenchymal transition (EMT) in malignant melanoma [8]. ICA-1S, the nucleoside analog of [4-(5-amino-4-carbamoylimidazol-1-yl)-2,3-dihydroxycyclopentyl] methyl dihydrogen phosphate was 1st reported as an inhibitor

for PKC-ι against melanoma cells in 2018 [8]. In vitro studies continue to show that ICA-1S is specific to PKC-ι, and the in vivo testing of malignant cell lines has continued to outline a decrease in malignant cell growth while normal cells are left largely unaffected [7–9]. Our previous virtual screening and kinase activity assay data suggested that ICA-1S is specific only to PKC-ι while having no effect on PKC-ζ [8]. PKC-ι is crucial in the tumorigenesis, progression, and survival of many cancers. More specifically, PKC-ι is involved in the rapid cell proliferation of human glioma cells, lung cancer cells, neuroblastoma cells, and prostate cancer cells. PKC-ι was first considered as a novel therapeutic target by Stallings-Mann et al. in 2006. They screened aurothiomalate (ATM) as a potent inhibitor of the interaction between the PB1 domain of PKC-ι and Par6. The half maximal inhibitory concentration (IC_{50}) of aurothiomalate ranged from 0.3 to 100 μM, indicating that some cell lines are insensitive. In addition, Aurothiomalate has the potential risk of developing gold toxicity even with low levels of the inhibitor, which is a common problem with gold therapy in rheumatoid arthritis. Therefore, there is a need for an effective and less toxic PKC-ι inhibitor [8]. In addition, our previous work has shown that ICA-1S did not affect normal melanocytes and prostate cells while decreasing the growth of melanoma and prostate cancer cells in vitro [7–10]. The pharmacokinetic properties of ICA-1S and its potential as a specific inhibitor for oncogenic PKC-ι without toxic effect on normal tissues [10], warrant the exploration of its potential chronic use as an oral therapeutic agent. To determine whether ICA-1S is a potential candidate for alternative therapy in various types of cancer, several key factors require testing. Here, the toxicity, pharmacokinetics, and therapeutic efficacy of ICA-1S in a chronic in vivo setting is tested while simultaneously testing the acute effects of hepatocyte and renal PTC toxicity using in vitro/in silico methods.

2. Results

2.1. Spectroscopy and Plasma Murine Drug Quantitation

Chronic ICA-IS (Figure 1) exposure appears to corroborate the linear kinetic behavior established in an acute toxicology study [10] with a half-life achieved within the first 24 h (Figure 2). ICA-IS also did not accumulate in any of the major organ tissues analyzed; tissue levels approached lower detection limits even at day 90 of repeated daily exposure.
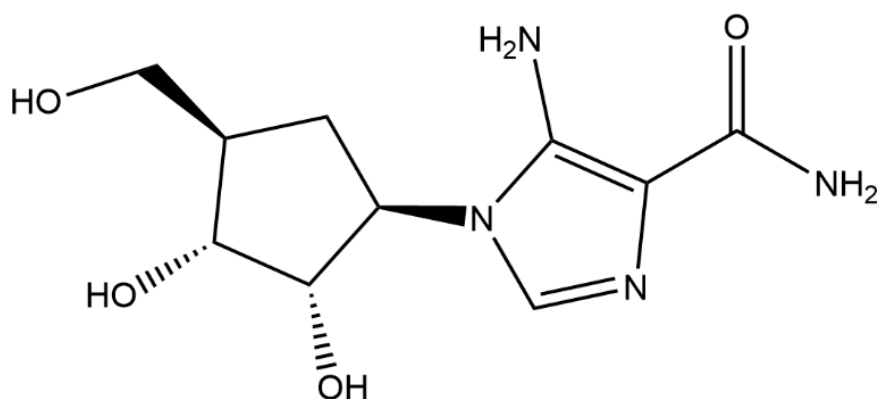
Figure 1. The chemical structure of ICA-1S, the inhibitor studied in this report. 5-amino-1-((1R,2S,3R,4R)-2-3-dihydroxy-4-(hydroxymethyl)cyclopentyl)-1H-imidazole-4-carboxamide, (ICA-1S) a PKC-ι specific inhibitor.
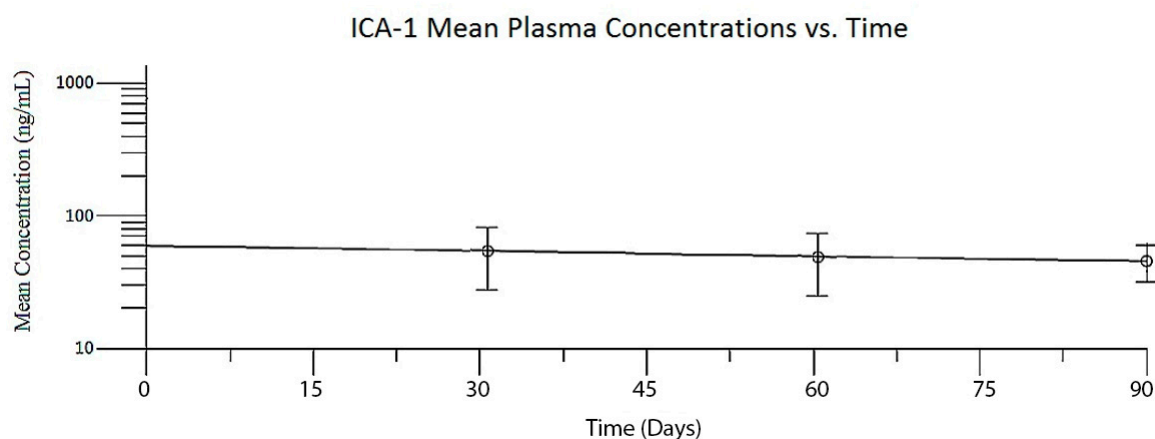
Figure 2. Mean plasma concentration of ICA-1S over time. A dose–response assessment of drug accumulation in blood serum. Animals were given an oral dose of 100 mg/kg of ICA-IS daily.

2.2. Chronic Toxicity

In a dose–response assessment, changes in organ function were measured by the levels of enzymes AST, GGT, Troponin I and CRP in blood serum, as indicated by colorimetric assay. Twenty animals were in each test group. Animals were given an oral dose of either 0 (control group), 50, 75, or 100 mg/kg of ICA-IS. Animals were sacrificed either 28, 60, or 90 days after treatment. Readings for CRP, AST, GGT, and Troponin I did not differ significantly compared to the control for any groups.

2.3. Predictive Toxicity with High-Content Imaging (HCI)

For predicting the potential organ toxicity of ICA-1S in humans, two organs that are frequently affected by compound-induced toxicity were selected: the liver and kidneys. In these organs, hepatocytes and renal proximal tubule cells (PTCs) are major targets of compound-induced toxicity, and therefore these two cell types are widely used for assessing liver and kidney toxicity [11,12]. Here, we used predictive in vitro/in silico methods [13,14] that employed HepaRG cells, which are considered to be one of the current, most suitable human hepatocyte models [11,15], or human primary renal proximal tubule cells (HPTCs), respectively.

The in vitro/in silico methods used here for predicting compound-induced direct hepatocyte toxicity [13] or renal PTC toxicity [14] in humans are based on the high-content imaging (HCI) of compound-treated cells in combination with phenotypic profiling. During phenotypic profiling, a large number of cellular phenotypic features, such as the cellular size and shape, nuclear DNA distribution, or changes in the intensity of stained cellular markers, were assessed to identify those phenotypic features where compound-induced changes best predict compound-induced toxicity in humans. To identify these changes, compound-induced phenotypes observed in vitro are compared to the in vivo toxicity of a compound with a machine learning algorithm using the annotated reference sets of compounds with known toxicity in humans. The predictive hepatocyte-specific method used here was established with an annotated reference set of 69 compounds and had a test sensitivity of 73% and specificity of 92% when a 30-dimensional predictive model was applied [13]. The predictive renal PTC-specific method was established with an annotated reference set of 42 chemicals and had a training sensitivity of 87% and a specificity of 89% when a 5-dimensional predictive model was applied (the predictive method used here is a modified version of the method described in [14]).

To predict the renal PTC toxicity of ICA-1S in humans, HPTCs pooled from three donors were treated with seven concentrations of ICA-1S ranging from 5 µM to 800 µM (for details see Section 4.6). After treatment, the analysis of cell numbers showed that ICA-1S was not cytotoxic for HPTCs (Figure 3) and HPTCs were imaged by HCI (Figure 4).
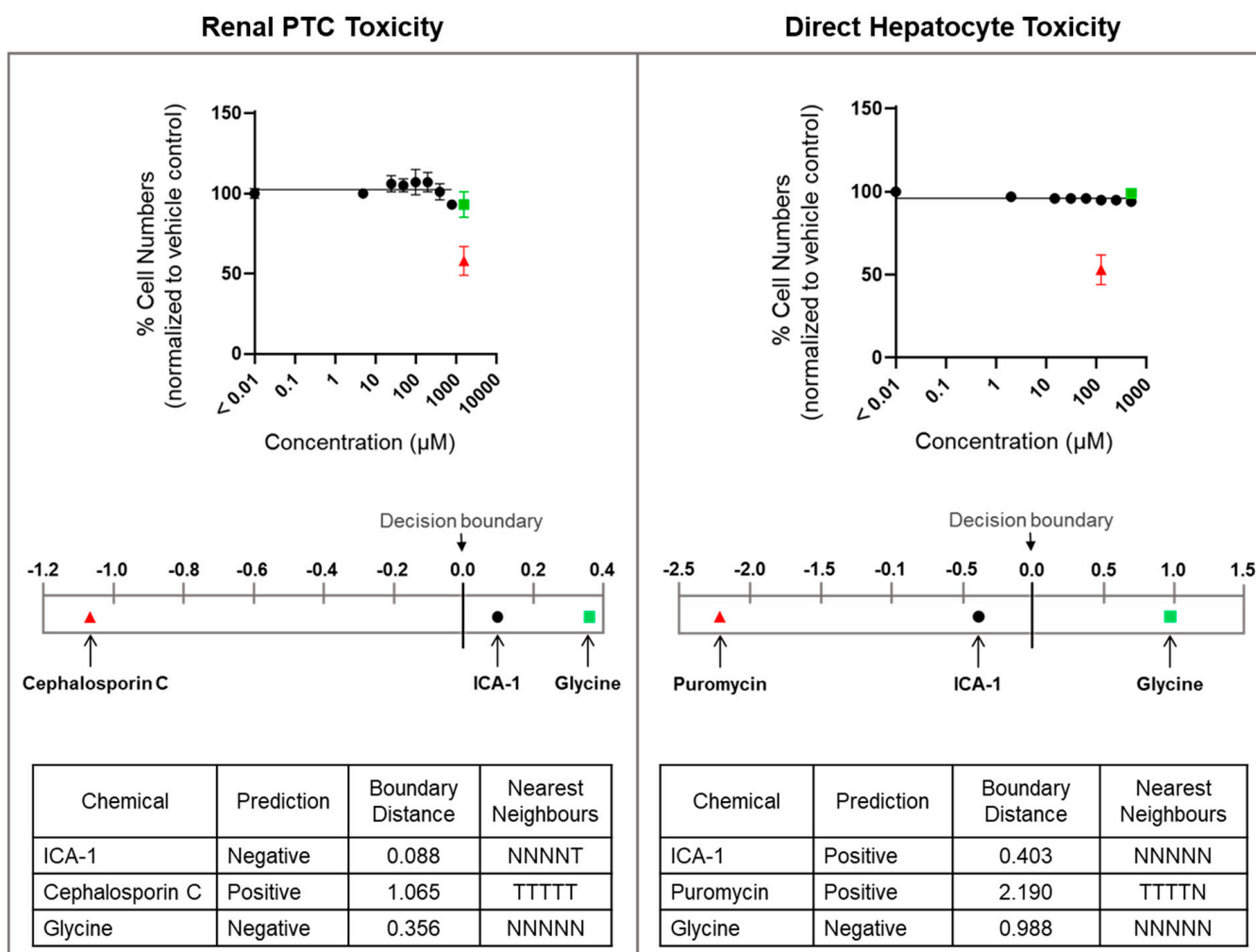
Figure 3. Analysis of ICA-1S-induced effects and toxicity prediction. The left-hand column summarizes the results relevant for the prediction of renal PTC toxicity in humans. All results were obtained using HPTCs. The right-hand column displays the results relevant for the prediction of direct hepatocyte toxicity in humans, and the results were obtained with HepaRG cells. The panels at the top show the average cell numbers (n = 3, +/− standard deviation) normalized to vehicle controls (vehicle controls set to 100%). All results for each tested concentration of ICA-1S are shown (black dots) as well as the fitted concentration–response curves. The first data point on the left is derived from the vehicle control. In addition, the results from the positive (red triangles) and negative (green squares) controls are shown. The panels in the middle show a 1-dimensional projection of the phenotypic feature space orthogonal to the plane of the decision boundary. The positions of the phenotypes induced by ICA-1S (black dots) and the positive (red triangles) and negative (green squares) controls are shown. The position of the decision boundary is indicated. The tables at the bottom display the predictions with respect to the renal PTC and hepatocyte toxicity of ICA-1S and the control chemicals, as well as the distances to the decision boundary in the phenotypic feature space. It is also indicated whether the chemicals that induced the 5 nearest-neighbor phenotypes were annotated as toxic (T) or not toxic (N) for the respective cell types in humans. The nearest-neighbor analysis was performed with the 42 or 69 reference chemicals used for establishing the respective predictive models.

Based on the 5-dimensional PTC-toxicity model's best predictive phenotypic features (Supplementary Table S1), the cellular phenotypes induced by ICA-1S and the positive (cephalosporin C) and negative (glycine) control compounds were calculated and mapped in the phenotypic feature space (Figure 3). In this space, PTC-toxic and PTC-non-toxic com-

pounds were separated by a decision hyperplane established in the predictive model with 42 reference compounds. The ICA-1S and glycine-induced phenotypes were positioned relative to the decision boundary in an area where the cellular responses are predictive of no direct PTC toxicity in humans (Figure 3). Therefore, based on their positions, ICA-1S and glycine were predicted to be non-toxic to human renal PTCs (Figure 3). In contrast, the phenotype induced by the positive control compound cephalosporin C was positioned in the area where cellular responses are predictive of direct PTC toxicity in humans, and therefore, cephalosporin C was predicted to be toxic for PTCs in humans.

Scale bar: 50 μM
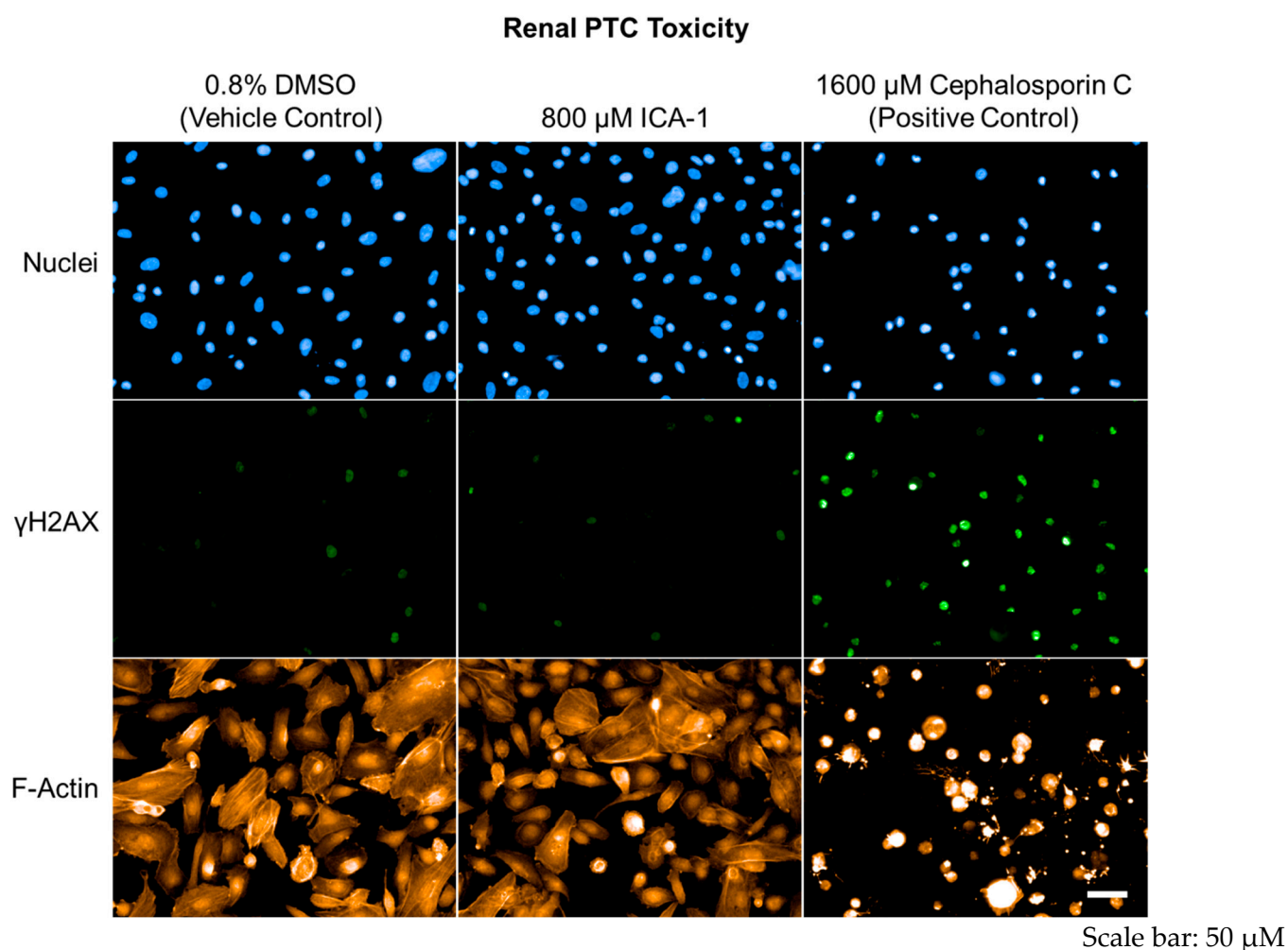
Figure 4. High-content imaging (HCI) results for HPTCs treated with ICA-1S and control chemicals. HPTCs were treated with the highest tested concentration of ICA-1S (800 μM), or with the vehicle control (0.8% DMSO). For comparison, HPTCs treated with the positive control (cephalosporin C) are shown. The images show the DAPI-stained cell nuclei (blue), the F-actin cytoskeleton (orange) and H2AX (green) detected by immunofluorescence. In each column, the same field of HPTCs is always shown.

As the ICA-1S phenotype was located relatively close to the decision boundary (in comparison to glycine, for instance), the negative prediction was made with medium confidence. The prediction of no renal PTC toxicity of ICA-1S is consistent with the analysis of the nearest neighbors in the phenotypic feature space (Figure 3). Four of the five nearest-neighbor phenotypes (induced by chemicals from the set of 42 reference compounds) were induced by compounds annotated as non-toxic for PTCs in humans (Figure 3). In summary, ICA-1S is predicted to be non-toxic for PTC in humans based on its location

in the phenotypic feature space, and this prediction is supported by the nearest-neighbor analysis and the absence of cytotoxicity for HPTCs.

ICA-1S-induced hepatocyte toxicity in humans was predicted using HepaRG cells treated with a range of seven ICA-1S concentrations ranging from 2 to 500 μM (for details see Section 4 Materials and Methods). After treatment, HepaRG cells were imaged by HCI (Figure 5). No cytotoxicity of ICA-1S for HepaRG cells was observed up to the highest concentration tested (Figure 3 and Supplementary Table S1).

Direct Hepatocyte Toxicity

Scale bar: 50 μM
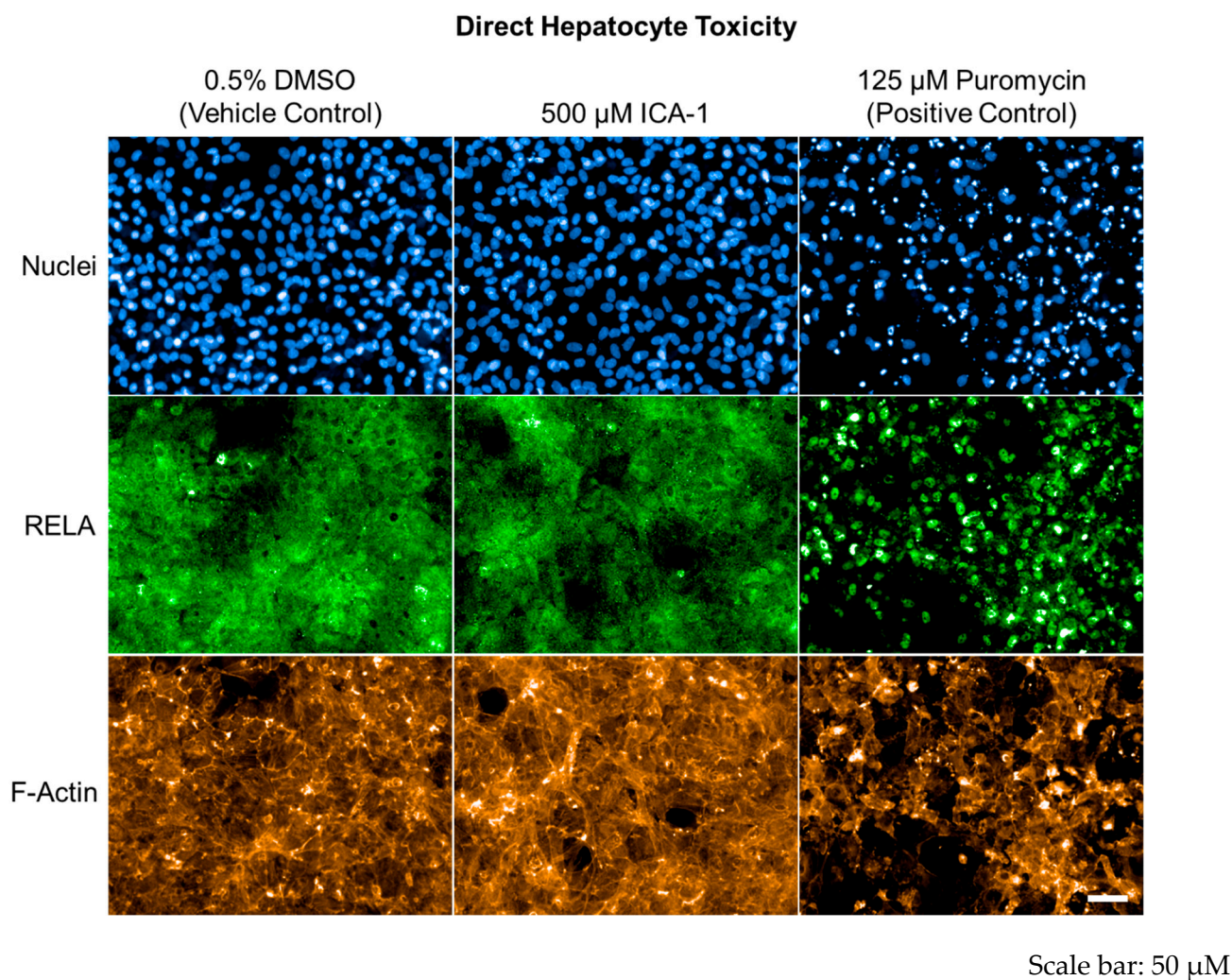
Figure 5. Images of HepaRG cells treated with ICA-1S and control chemicals. HepaRG cells were treated with the highest concentration of ICA-1S (500 μM) applied to this cell type, or with the vehicle control (0.5% DMSO). For comparison, HepaRG cells treated with the positive control (puromycin) are shown. The images show the DAPI-stained cell nuclei (blue), the F-actin cytoskeleton (orange) and RELA (green) detected by immunofluorescence. In each column, the same field of HepaRG cells is always shown. Scale bar: 50 μM.

The 30 best predictive phenotypic features (Supplementary Table S1) were evaluated to map the cellular phenotypes induced by ICA-1S and the control compounds in the phenotypic feature space (Figure 3). Together with the phenotype induced by the positive control compound puromycin, the ICA-1S-induced phenotype mapped to the area where cellular responses are predictive of direct toxicity for hepatocytes in humans (Figure 3). Based on these positions, ICA-1S and puromycin are predicted to be toxic for hepatocytes in humans (Figure 3). In contrast, the negative control compound glycine was predicted to

be non-toxic for hepatocytes in humans. The ICA-1S-induced phenotype was a moderate distance from the decision boundary.

However, all five nearest-neighbor phenotypes in the phenotypic feature space were induced by chemicals (from the reference set of 69 chemicals) annotated as non-toxic for hepatocytes in humans (Figure 3; the chemicals that induced the 5 nearest-neighbor phenotypes were induced by nicotine, aspartame, gentamycin sulfate, naloxone and glutathione). Based on the inconsistency between the position with respect to the decision boundary and the nearest-neighbor analysis, the confidence in the positive prediction is low. It should also be noted that ICA-1S had no cytotoxicity and did not induce the cytoplasmic-to-nuclear translocation of RELA in HepaRG cells (Supplementary Table S1), as is typical of compounds directly toxic for hepatocytes in humans [13]; see also the cytoplasmic-to-nuclear translocation of RELA-induced here by the positive control puromycin (Figure 5). Thus, these results did not provide evidence for the hepatocyte toxicity of ICA-1S.

3. Discussion

This study sought to investigate the potential of ICA-1S as a therapeutic agent by evaluating the toxicity of ICA-1S on healthy tissues in mice and its potential predicted toxic effects on healthy human liver and kidney tissues. Our findings indicate that the therapeutic compound ICA-1S not only lacks any toxic effects in animal tissues, as evidenced by no accumulation being present in any of the organs tested, but also shows promising results in predictive analysis for human tissue. With no accumulation of ICA-1S in any of the organs tested, our findings indicate that the therapeutic compound ICA-1S shows no toxic effect in animal tissues. While there is no current human-specific tissue data available, predictive analysis shows promising results, and although one measure of the predictive analysis found some potential for toxicity to hepatocyte cells, the confidence in that prediction was low and further analysis found no cytoplasmic-to-nuclear translocation in those cells.

Furthermore, In comparison to other pharmaceuticals [10], preliminary findings would, at a minimum, warrant further research and exploration of ICA-1S as a potential specific inhibitor [16–18]. Cumulatively, results from the current and prior studies indicate ICA-1S is an inhibitor specific to the oncogenetic protein PKC-ι, and its use could significantly reduce the prostate cancer growth rate while leaving healthy tissue relatively unaffected [10].

These results suggest that ICA-1S could be a very useful therapeutic in patients with prostate cancer or other slow-growing tumors with similar mutations. Since ICA-1S does not target anti-androgens like some therapeutics currently in use [19], it may also have value as part of a regimen that uses a combination of drugs. Given these pharmacokinetic properties described, ICA-1S could potentially be used as an oral therapeutic either with or in place of some therapeutics currently in use, and further efforts should be made to develop the compound for clinical use.

4. Materials and Methods

4.1. Chronic Toxicity

An oral up-and-down (UDP) and dose–response procedure from a previously published acute study [10] was implemented to estimate the median lethal dose (LD_{50}) and dose response in mice. One animal at a time was tested, with the response of each animal to the test substance determining whether the next animal received a higher or lower dose. All animal experimental procedures were reviewed and approved by the Institutional Animal Care and Use Committee of University of South Florida, Tampa, FL, USA (IACUC number IS00005822) in accordance with the US NIH Guidelines for animal research.

4.2. Dose–Response

ICA-1S was purchased from Therachem Research Medilab (catalog number #TRM-01785-5, Jaipur, India). The repeated dose toxicity of ICA-1S was established using 120 mice at 3 time points and in 4 treatment groups, as follows: Group 1: Vehicle Control; Group 2:

ICA-1S (50 mg/kg); Group 3: ICA-1S (75 mg/kg); Group 4: ICA-1S (100 mg/kg). Each group had five males and five females. ICA-1S was administered daily in graduated doses to three groups of experimental animals, one dose level per group, and each experimental group was replicated for 3 different time points, 28 days, 60 days, and 90 days. The dose volume did not exceed 1 mL/100 g body weight and the variability in test volume was minimized by adjusting the concentration to ensure a constant volume at all dose levels. During administration, animals were observed closely each day for signs of toxicity, which included changes in their skin, fur, eyes, mucus membranes, the occurrence of secretions and excretions and autonomic activity (e.g., lacrimation, piloerection, pupil size changes, changes in gait, posture, or an unusual respiratory pattern). Animals were euthanized by placement in a carbon dioxide chamber 24 h after the final ICA-1S administration (on day 28, 60, or 90, depending on treatment group), after which they sustained cervical dislocation as a secondary means of euthanasia. Blood and tissue were collected. The functional perturbation of the liver, kidneys and heart was tested by measuring the serum levels of the enzymes aspartate aminotransferase (AST) (catalog number #K753-100 from BioVision, Milpitas, CA, USA), gamma-glutamyl transpeptidase (GGT) (catalog number #K784-100 from BioVision, Milpitas, CA, USA), C-reactive protein (CRP) (catalog number #EK294 from Bioocean, Shoreview, MN, USA), and troponin (catalog number #ABIN1117615 from Elabscience Biotechnology Inc., Houston, TX, USA). Tissues collected were assessed for gross pathology and morphology.

4.3. Plasma Murine Drug Quantitation (Pharmacokinetics and Bioavailability)

Plasma levels were measured to evaluate compound half-life and other typical characteristics required for the evaluation of a drug candidate. Tissue levels of several organs of interest were also evaluated to look at the bio-distribution of the compound and measure any accumulation of the compound in organs. The following organs: the liver, kidneys, heart and brain, were collected during the sacrifice procedure.

4.4. LC-MS-MS (Liquid Chromatography Tandem Mass Spectrometry)

To form calibrations sets for plasma and tissue analysis, the methodology from a prior acute study [10] was mirrored in which mouse plasma spiked with known concentrations of unphosphorylated ICA-1S was added to a Sirocco (Waters Corporation, Milford, MA, USA) protein precipitation plate containing a solvent of acetonitrile and methanol. The plate was vortexed briefly and then placed in a centrifuge (Eppendorf—Hamburg, Germany) to stimulate the pass-through of the eluent onto a collection plate. The eluent was then evaporated with an Ultravap system (Porvair Sciences, Wrexham, UK). Samples were reconstituted with 0.1% acetic acid and vortexed before instrument analysis. The untreated (blank) tissue of each organ was also spiked with known concentrations of ICA-1S and homogenized in ice-cold 0.1% acetic acid at a concentration of 10 mL/g. After centrifugation, a 1:1 solvent consisting of acetonitrile and methanol was added to the supernatant and the samples were vortexed, centrifuged, and evaporated after centrifugation. Samples were reconstituted with 0.1% acetic acid and vortexed prior to instrument analysis [20].

Samples were injected into a Thermo Accela Ultra-High Performance Liquid Chromatography system coupled to a Thermo TSQ Quantum Tandem Mass Spectrometer (Thermo Electron, San Jose, CA, USA). Gradient elution was achieved with mobile phases of water and methanol, both containing 0.1% acetic acid. A Phenomenex Luna reverse phase C18 column (Phenomenex, Torrance, CA, USA) was used to separate compounds. The mass spectrometry system employs heated electrospray ionization (H-ESI) in the source followed by the selected reaction monitoring (SRM) of the target compound. The SRM transition was monitored in positive ion mode for a quantitation of $240.100 \rightarrow 110.054$ ICA-1S. The assay had a linear range from 5 to 2500 ng/mL for plasma and 5–5000 ng/mL in tissue.

4.5. Cell Culture

HepaRG cells were purchased from Thermo Fisher Scientific (Singapore). They were seeded at a density of 200,000 cells/cm^2 into 384-well black plates with transparent bottoms (Greiner, Kremsmunster, Austria), coated with rat tail collagen I (Advanced BioMatrix, San Diego, CA, USA). For 24 h, cells were cultivated in William's E Medium (Thermo Fisher Scientific), supplemented with HepaRG Thaw, Plate & General Purpose Medium Supplement (Thermo Fisher Scientific) and 1% GlutaMAX (Thermo Fisher Scientific), followed by cultivation for 7 days in William's E Medium supplemented with HepaRG Tox Medium Supplement (Thermo Fisher Scientific) and 1% GlutaMAX. Treatment with ICA-IS was performed on day 7.

Human primary renal proximal tubule cells (HPTCs) were purchased from the American Type Culture Collection (ATCC, Manassas, VA, USA) and cultured in a renal epithelial cell basal medium (ATCC) supplemented with a renal epithelial cell growth kit (ATCC) and 1% penicillin/streptomycin (Thermo Fisher Scientific). HPTCs at passage five pooled from three different donors were used for compound screening. Cells were seeded at a density of 50,000 cells/cm^2 into 384-well black plates with transparent bottoms, 3 days before treatment with ICA-IS. All cells were tested with the Lonza MycoAlert Plus mycoplasma detection kit (Lonza Group AG, Basel, Switzerland) to check for contamination, and all results were negative.

4.6. Compound Treatment and High-Content Imaging (HCI)

To predict hepatocyte toxicity in humans, HepaRG cells were treated with seven concentrations of ICA-1S dissolved in 100% dimethylsulfoxide (DMSO, vehicle): 2, 15, 31, 62, 125, 250, and 500 μM (n = 3). DMSO (0.5%) in a cell culture medium was used as the vehicle control. The positive and negative plate controls were 125 μM of puromycin and 500 μM of glycine, respectively. To predict renal proximal tubule cell (PTC) toxicity in humans, HPTCs were treated with seven concentrations of ICA-1S dissolved in 100% DMSO: 5, 25, 50, 100, 200, 400, and 800 μM (n = 3). DMSO (0.8%) in a cell culture medium was used as the vehicle control; 1600 μM of cephalosporin C and 1600 μM of glycine were used as positive and negative plate controls, respectively.

Cells were exposed to ICA-IS for 16 h. Subsequently, cells were fixed for 10 min with 3.7% formaldehyde in phosphate-buffered saline (PBS), followed by washing with PBS and blocking with PBS containing 5% bovine serum albumin and 0.2% Triton-X-100. For the immunostaining of HPTCs, a primary mouse monoclonal anti-γH2AX antibody (Abcam, Cambridge, MA, USA) and a secondary goat anti-mouse antibody conjugated to Alexa 488 (Thermo Fisher Scientific) were used. The immunostaining of HepaRG cells was performed with a rabbit polyclonal anti-RELA antibody (Abcam), followed by incubation with an Alexa 488-conjugated goat anti-rabbit antibody (Thermo Fisher Scientific). In both cell types, F-actin was detected with rhodamine phalloidin (Thermo Fisher Scientific). Cell nuclei were stained with 4′, 6-diamidino-2-phenylindole dihydrochloride (DAPI, Merck Millipore, Darmstadt, Germany) and entire cells were stained with HCS Cell Mask Deep Red Stain (Thermo Fisher Scientific). Automated imaging was performed with a 20× objective and an Operetta CLS high-content imaging system (PerkinElmer Inc., Waltham, MA, USA) equipped with Harmony high-content imaging and analysis software (version 4.6.2107.265, PerkinElmer Inc.). Nine sites per well were imaged and four channels were used for the different fluorochromes.

4.7. Quantification of Cell Numbers

Cell numbers were estimated using the numbers of DAPI-stained cell nuclei. Quantitative image analysis was performed with the Columbus Image Data Storage and Analysis System (PerkinElmer Inc.). All results were normalized to the respective vehicle controls. Concentration–response curves were plotted with Prism software (Version 8.4.3, GraphPad Software, San Diego, CA, USA). Based on the positive and negative plate controls, all Z′ values [21] were 1.0 with respect to cell numbers.

4.8. Prediction of Hepatocyte Toxicity in Humans

The hepatocyte toxicity of ICA-1S was predicted using the model for predicting direct hepatocyte toxicity in humans [13]. Briefly, this predictive model [13] was established with a reference set of 69 annotated chemicals for which evidence was available in the published literature on the chemicals' direct toxicity for hepatocytes in humans; 22 of these compounds were annotated as directly toxic and the remaining 47 as not directly toxic for hepatocytes in vivo in humans. During the establishment of this model, the phenotypic changes induced by the 69 reference chemicals in HepaRG cells were analyzed using the HCI data of compound-treated HepaRG cells. The compound-induced phenotypic changes analyzed included changes in cellular and nuclear size and shape, in nuclear DNA distribution, and in the intensity of stained cellular markers at various cellular regions. The input of this model was the cellular response at 500 μM interpolated from the fitted log-logistic dose–response curves. This metric was found to be more predictive than the potency metrics of the response curves [22]. Based on an unbiased analysis of 210 phenotypic features, 30 phenotypic features were identified to create a model with the highest balanced accuracy (defined as the average of specificity and sensitivity) for correctly classifying the 69 reference chemicals [13]. These 30 phenotypic features were related to the F-actin cytoskeleton, RELA (RELA proto-oncogene, NF-kB subunit; also known as NF-kappa B p65), nuclear DNA distribution, and other nuclear features (Supplementary Table S2). Predictive performance was determined using 10-fold cross-validation, and the model had a test specificity, sensitivity, and balanced accuracy of 92%, 73%, and 83%, respectively [13]. Here, this model [13] was applied for the analysis of the HCI data of ICA-1S-treated HepaRG cells and for the hepatocyte toxicity prediction of ICA-1S. The ICA-1S-induced response at 500 μM based on the fitted dose–response curve was used as input, and the prediction made based on ICA-1S-induced changes in the previously identified 30 most predictive phenotypic features (Supplementary Table S2). The processing of HCI image data, cell segmentation, and phenotypic feature extraction was performed using the cellXpress software [23].

4.9. Determining the Nuclear Translocation of RELA

Independent from the analyses of RELA features performed during the analysis of 30 predictive phenotypic features for predicting direct hepatocyte toxicity in humans (Supplementary Table S1), the cytoplasmic–nuclear translocation of RELA was also analyzed with the Columbus Image Data Storage and Analysis System (PerkinElmer Inc.). This system was used to quantify the nuclear and cytoplasmic intensities of RELA and their ratios. All results were normalized to the respective vehicle controls. Based on the positive and negative plate controls, the Z' value [21] was 0.57 with respect to the cytoplasmic–nuclear translocation of RELA.

4.10. Prediction of Renal PTC Toxicity in Humans

Renal PTC toxicity was predicted with a modified version of the model for predicting PTC toxicity in humans [14]. Similar to the model for predicting hepatocyte toxicity, the model for predicting renal PTC toxicity was developed by performing an unbiased analysis of 172 compound-induced changes of cellular phenotypic features in order to identify those phenotypic features to construct a model with the highest balanced accuracy for predicting compound-induced PTC toxicity in humans. The modified version of the model was calibrated using 42 annotated reference chemicals [14]. Of these reference chemicals, 23 were annotated as directly toxic and the remaining 19 were annotated as not directly toxic for PTC in humans. The final predictive model was constructed from 5 phenotypic features. The 5 features used for predicting renal PTC toxicity included 3 features related to the F-actin cytoskeleton and 2 combined features (related to DNA and F-actin or DNA and γH2AX; Supplementary Table S2), consistent with previous findings [14]. This model used the responses at 800 μM, as interpolated from the fitted log-logistic concentration–response curves, as input. It had a test specificity, sensitivity, and balanced accuracy of 89%, 87%,

and 88%, respectively, as determined by using 10-fold cross-validation. For predicting the renal PTC toxicity of ICA-1S in humans, the cellular response at 800 μM based on the fitted concentration–response curve was used as input. The processing of HCI image data, cell segmentation, and phenotypic feature extraction was performed with the cellXpress software [23].

Supplementary Materials: The following supporting information can be downloaded at: https://www.mdpi.com/article/10.3390/ddc3020022/s1; Table S1: Effects of ICA-1S on HepaRG cell numbers and cytoplasmic-to-nuclear translocation of RELA; Table S2: Predictive phenotypic features.

Author Contributions: Conceptualization, M.A.-D.; methodology, C.A.A., W.S.R., S.B., D.Z., J.A.M., J.K.C.C. and M.B.; validation, C.A.A., W.S.R., J.A.M., J.K.C.C. and D.Z.; formal analysis, C.A.A., S.B. and W.S.R.; investigation C.A.A., S.B., W.S.R., J.A.M., J.K.C.C. and D.Z.; resources, M.A.-D.; data curation, C.A.A., W.S.R. and S.B.; writing—original draft preparation, W.S.R. and C.A.A.; writing—review and editing, W.S.R., M.A.-D., D.Z.; supervision, M.A.-D., funding acquisition, M.A.-D. All authors have read and agreed to the published version of the manuscript.

Funding: Funding was received from the Leo and Anne Albert Charitable Trust and Ella Owens Medical Research Foundation to perform the pre-clinical studies.

Institutional Review Board Statement: All animal experimental procedures were reviewed and approved by the Institutional Animal Care and Use Committee of University of South Florida, Tampa, FL, USA (IACUC number IS00005822) in accordance with the US NIH Guidelines for animal research.

Informed Consent Statement: Not applicable.

Data Availability Statement: The original contributions presented in the study are included in the article/Supplementary Materials. Further inquiries can be directed to the corresponding author.

Acknowledgments: The Authors would like to acknowledge the generous contributions made by Gene Pranzo and The Leo and Anne Albert Charitable Trust, along with The William and Ella Owens Medical Research Foundation for their continued and instrumental financial support.

Conflicts of Interest: C.A. Apostolatos, W.S. Ratnayake, S. Breedy, James Alastair Miller, Marie Bourgeois, and Mildred Acevedo-Duncan declare no conflicts of interest. Jacqueline Kai Chin Chuah and Daniele Zink are an employee and a shareholder, respectively, of Cellbae Pte Ltd., which conducted the nephrotoxicity and hepatotoxicity assays on ICA-1S described in this study. The funders had no role in the design of the study; in the collection, analyses, or interpretation of data; in the writing of the manuscript; or in the decision to publish the results.

References

1. Win, H.Y.; Acevedo-Duncan, M. Role of Protein Kinase C-iota in Transformed Non-malignant RWPE-1 Cells and Androgen-independent Prostate Carcinoma DU-145 Cells. *Cell Prolif.* **2009**, *42*, 182–194. [CrossRef] [PubMed]
2. Eder, A.M.; Sui, X.; Rosen, D.G.; Nolden, L.K.; Cheng, K.W.; Lahad, J.P.; Kango-Singh, M.; Lu, K.H.; Warneke, C.L.; Atkinson, E.N.; et al. Atypical PKCiota Contributes to Poor Prognosis through Loss of Apical-Basal Polarity and Cyclin E Overexpression in Ovarian Cancer. *Proc. Natl. Acad. Sci. USA* **2005**, *102*, 12519–12524. [CrossRef] [PubMed]
3. Ratnayake, W.S.; Apostolatos, A.H.; Ostrov, D.A.; Acevedo-Duncan, M. Two Novel Atypical PKC Inhibitors; ACPD and DNDA Effectively Mitigate Cell Proliferation and Epithelial to Mesenchymal Transition of Metastatic Melanoma While Inducing Apoptosis. *Int. J. Oncol.* **2017**, *51*, 1370–1382. [CrossRef] [PubMed]
4. Patel, R.; Win, H.; Desai, S.; Patel, K.; Matthews, J.A.; Acevedo-Duncan, M. Involvement of PKC-ι in Glioma Proliferation. *Cell Prolif.* **2008**, *41*, 122–135. [CrossRef] [PubMed]
5. Paul, A.; Gunewardena, S.; Stecklein, S.R.; Saha, B.; Parelkar, N.; Danley, M.; Rajendran, G.; Home, P.; Ray, S.; Jokar, I.; et al. PKCλ/ι Signaling Promotes Triple-Negative Breast Cancer Growth and Metastasis. *Cell Death Differ.* **2014**, *21*, 1469–1481. [CrossRef] [PubMed]
6. Chalhoub, N.; Baker, S.J. PTEN and the PI3-Kinase Pathway in Cancer. *Annu. Rev. Pathol.* **2009**, *4*, 127–150. [CrossRef] [PubMed]
7. Apostolatos, A.H.; Ratnayake, W.S.; Win-Piazza, H.; Apostolatos, C.A.; Smalley, T.; Kang, L.; Salup, R.; Hill, R.; Acevedo-Duncan, M. Inhibition of Atypical Protein Kinase C-ι Effectively Reduces the Malignancy of Prostate Cancer Cells by Downregulating the NF-κB Signaling Cascade. *Int. J. Oncol.* **2018**, *53*, 1836–1846. [CrossRef] [PubMed]
8. Ratnayake, W.S.; Apostolatos, C.A.; Apostolatos, A.H.; Schutte, R.J.; Huynh, M.A.; Ostrov, D.A.; Acevedo-Duncan, M. Oncogenic PKC-ι Activates Vimentin during Epithelial-Mesenchymal Transition in Melanoma; a Study Based on PKC-ι and PKC-ζ Specific Inhibitors. *Cell Adhes. Migr.* **2018**, *12*, 447–463. [CrossRef] [PubMed]

9. Ratnayake, W.S.; Apostolatos, C.A.; Breedy, S.; Dennison, C.L.; Hill, R.; Acevedo-Duncan, M. Atypical PKCs Activate Vimentin to Facilitate Prostate Cancer Cell Motility and Invasion. *Cell Adhes. Migr.* **2021**, *15*, 37–57. [CrossRef] [PubMed]

10. Apostolatos, A.H.; Apostolatos, C.A.; Ratnayake, W.S.; Neuger, A.; Sansil, S.; Bourgeois, M.; Acevedo-Duncan, M. Preclinical Testing of 5-Amino-1-((1R,2S,3S,4R)-2,3-Dihydroxy-4-Methylcyclopentyl)-1H-Imidazole-4-Carboxamide: A Potent Protein Kinase C-ι Inhibitor as a Potential Prostate Carcinoma Therapeutic. *Anticancer Drugs* **2019**, *30*, 65–71. [CrossRef] [PubMed]

11. Gómez-Lechón, M.J.; Tolosa, L.; Conde, I.; Donato, M.T. Competency of Different Cell Models to Predict Human Hepatotoxic Drugs. *Expert Opin. Drug Metab. Toxicol.* **2014**, *10*, 1553–1568. [CrossRef] [PubMed]

12. Tiong, H.Y.; Huang, P.; Xiong, S.; Li, Y.; Vathsala, A.; Zink, D. Drug-Induced Nephrotoxicity: Clinical Impact and Preclinical in Vitro Models. *Mol. Pharm.* **2014**, *11*, 1933–1948. [CrossRef]

13. Hussain, F.; Basu, S.; Heng, J.J.H.; Loo, L.-H.; Zink, D. Predicting Direct Hepatocyte Toxicity in Humans by Combining High-Throughput Imaging of HepaRG Cells and Machine Learning-Based Phenotypic Profiling. *Arch. Toxicol.* **2020**, *94*, 2749–2767. [CrossRef] [PubMed]

14. Su, R.; Xiong, S.; Zink, D.; Loo, L.-H. High-Throughput Imaging-Based Nephrotoxicity Prediction for Xenobiotics with Diverse Chemical Structures. *Arch. Toxicol.* **2016**, *90*, 2793–2808. [CrossRef] [PubMed]

15. Andersson, T.B.; Kanebratt, K.P.; Kenna, J.G. The HepaRG Cell Line: A Unique in Vitro Tool for Understanding Drug Metabolism and Toxicology in Human. *Expert Opin. Drug Metab. Toxicol.* **2012**, *8*, 909–920. [CrossRef] [PubMed]

16. Murray, N.R.; Fields, A.P. Atypical Protein Kinase C Iota Protects Human Leukemia Cells against Drug-Induced Apoptosis. *J. Biol. Chem.* **1997**, *272*, 27521–27524. [CrossRef] [PubMed]

17. Pillai, P.; Desai, S.; Patel, R.; Sajan, M.; Farese, R.; Ostrov, D.; Acevedo-Duncan, M. A Novel PKC-ι Inhibitor Abrogates Cell Proliferation and Induces Apoptosis in Neuroblastoma. *Int. J. Biochem. Cell Biol.* **2011**, *43*, 784–794. [CrossRef] [PubMed]

18. Xie, J.; Guo, Q.; Zhu, H.; Wooten, M.W.; Mattson, M.P. Protein Kinase C Iota Protects Neural Cells against Apoptosis Induced by Amyloid Beta-Peptide. *Brain Res. Mol. Brain Res.* **2000**, *82*, 107–113. [CrossRef] [PubMed]

19. Semenas, J.; Dizeyi, N.; Persson, J.L. Enzalutamide as a Second Generation Antiandrogen for Treatment of Advanced Prostate Cancer. *Drug Des. Devel Ther.* **2013**, *7*, 875–881. [CrossRef] [PubMed]

20. Götze, L.; Hegele, A.; Metzelder, S.K.; Renz, H.; Nockher, W.A. Development and Clinical Application of a LC-MS/MS Method for Simultaneous Determination of Various Tyrosine Kinase Inhibitors in Human Plasma. *Clin. Chim. Acta* **2012**, *413*, 143–149. [CrossRef] [PubMed]

21. Zhang, J.H.; Chung, T.D.; Oldenburg, K.R. A Simple Statistical Parameter for Use in Evaluation and Validation of High Throughput Screening Assays. *J. Biomol. Screen.* **1999**, *4*, 67–73. [CrossRef] [PubMed]

22. Miller, J.A.; Loo, L.-H. Optimum Concentration-Response Curve Metrics for Supervised Selection of Discriminative Cellular Phenotypic Endpoints for Chemical Hazard Assessment. *Arch. Toxicol.* **2020**, *94*, 2951–2964. [CrossRef] [PubMed]

23. Laksameethanasan, D.; Tan, R.; Toh, G.; Loo, L.-H. cellXpress: A Fast and User-Friendly Software Platform for Profiling Cellular Phenotypes. *BMC Bioinform.* **2013**, *14* (Suppl. S16), S4. [CrossRef] [PubMed]